Retrieval of Single-Doppler Radar Wind Field by Nonlinear Approximation

ZHAO Kun*[1] (赵 坤), LIU Guoqing[2] (刘国庆), GE Wenzhong[1] (葛文忠), DANG Renqing[1] (党人庆), and Takao TAKEDA[3]

[1] *Department of Atmospheric Sciences, Nanjing University, Nanjing* 210093

[2] *Department of Mathematics, Nanjing University of Technology, Nanjing* 210009

[3] *Institutes for Hydrospheric Atmospheric Sciences, Nagoya University,* 464-8601 *Japan*

(Received August 5, 2002; revised December 20, 2002)

ABSTRACT

The methods employed in recent years to retrieve vector wind information from single-Doppler radar observation are reviewed briefly. These methods are based on a linearity hypothesis for the wind field, so the retrieved wind field is sometimes negatively affected by the non-linearity of wind. This paper proposes a new method based on a non-linear approximation technique. This method, which relies on the piecewise smooth property of the wind field and makes full use of the radar velocity data, is applied to two cases of the Huaihe River Basin Energy and Water Cycle Experiment (HUBEX) in 1998. Checked against the wind field observed by dual-Doppler radar, the retrieved wind field by the method presented in this paper yields a relatively accurate horizontal vector wind field with high resolution, as well as a reasonable estimate of the magnitude of vertical velocity.

Key words: nonlinear approximation, piecewise smooth wind field, basis function

1. Introduction

Modern Doppler radars have the ability to scan large volumes of the atmosphere at high spatial and temporal resolutions, but the direct measurement is limited to the velocity component in the direction of the radar beam. In brief, the difficulty is that one would like to know the three-dimensional wind field, but single-Doppler radar observation yields only the wind component along radius. The velocity perpendicular to the axis of the radar beam is often critical in some hazardous weather situations (especially low-level wind shear associated with convective downbursts). The complete wind fields are necessary to allow initialization of a numerical model that could predict hazardous weather conditions in advance.

Every attempt to obtain the vector field from a single-Doppler radar observation must handle the data field with additional hypotheses or simplifications. In a study by Peace et al. (1969), the main hypothesis is that the echo region moves across the radar field of view with little modification of the wind field structure, to such an extent that two radar explorations separated in time can be viewed as a simultaneous exploration by two distant radars. Many other methods assume a simplifying property of the wind field itself, rather than its time variation. Lhermitte and Atlas (1961) suggested the VAD (Velocity Azimuth Display) method and showed how the mean horizontal wind magnitude and direction can be retrieved from radial velocity data around horizontal circles centered along the vertical axis of the radar site. This and other similar techniques, such as volume velocity processing (VVP) (Waldteufel and Corbin, 1979), extended VAD (Srivastava et al., 1986; Matejka and Srivastava, 1991), and double VAD (Scialom and Testud, 1986) assume linearity in the observed wind fields and are best suited for the estimation of large-scale wind fields in a stratiform cloud system. Bai et al. (2001) analyzes the Error of expanded VAD technique and illustrates that the fitting harmonic curve of half VAD technique and TVAD technique can give the characteristic of the large-scale wind field in the calculated area. The band velocity processing (BVP) technique is a modification of the VVP technique that can be employed to examine the three-dimensional wind fields of phenomena

*E-mail: zaokun@263.net

remote from the radar, assuming that the feature is two-dimensional. BVP analyses have been successfully performed on cold-frontal rainbands (Johnston et al., 1990), snow bands (Marwitz, 1990), and a severe squall line (Klimowski and Marwitz. 1990). The velocity azimuth processing method (VAP) is provided to retrieve the horizontal wind field (Tao, 1992), assuming that the wind vector is equal at a neighboring azimuth. Bai and Tao (2000) modified the data pre-processing technique of the VAP method. Wei et al. (1998) provided a feasible algorithm to solve the problem of ill matrices in the linear equations of the VVP method and to improve the degree of accuracy of the method. Liu and Tao (1999), using a polar coordinate divergence method, retrieve divergence from single-Doppler radar velocity data in polar coordinates.

Another single-Doppler analysis technique has been proposed utilizing the temporal correlation of reflectivity and velocity signatures to indicate horizontal wind (Smythe and Zrnic 1983; Tuttle and Foote 1990). This method is known as Tracking Radar Echoes by Correlation (TREC), which indicates the motion of the correlated property, which may be the result of advection or propagation, and not necessarily the true wind. Although the results from TREC analyses indicate that it is a viable analysis technique of wind fields, it requires a short interval between two radar observations, or else the precision of the retrieved wind fields will be much degraded.

Recently, single-Doppler analysis techniques with integrated dynamic models have been developed for the retrieval of thermodynamic parameters in addition to the full wind, such as retrieval by the adjoint technique with a full numerical model (Sun et al., 1991; Liou et al., 1991), retrieval by the simple adjoint method (Qiu and Xu, 1992; Xu Qin et al., 1994. 1995) etc, and others. These methods contribute to the advancement of single-Doppler wind retrieval and show promise for increasing the amount of data recoverable from single-Doppler datasets, but they bring extra assumptions associated with the numerical models, which may degrade the accuracy of the retrieved wind.

Of the above methods, the VVP method is used most extensively. But as we know, the VVP method does not work properly when the samples of one volume number less than a few hundred and the VVP method has a low resolution. Furthermore, it is much affected by non-linearity in the wind field and it has a large error for the vertical speed.

In order to improve the wind retrieval precision and resolution, this paper proposes a new method based on a nonlinear approximation technique (NA) with the assumption that the wind field is piecewise smooth. The NA method was initially applied to a signal process field by Coifman et al. (1992); since it has been extended by many scholars such as Chapelle et al. (1999), Cohen and d'Ales (1997), Gorodnitsky and Rao (1997), Girosi (1998), Evgeniou (2000), Vapnik and Chervonenkis (1971) , Vapnik (1995, 1998a, b), and Vapnik and Mukherjee (2000). Here, we apply this method to two cases of the HUBEX experiment in 1998, and the retrieved wind field is compared with dual-Doppler radar data. The results show that better retrieval and higher resolution of the three-dimensional wind field can be obtained with the method given in this paper. The experiments provide useful observational information for studying the inner flow structure.

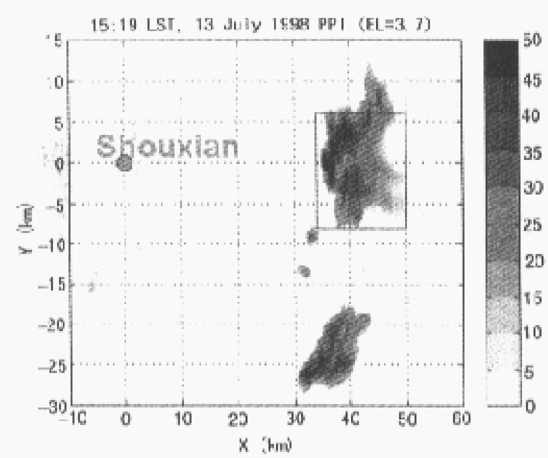

Fig. 1. The reflectivity (PPI, EL=3.7° of Shouxian radar at 1519 LST 13 July 1998.

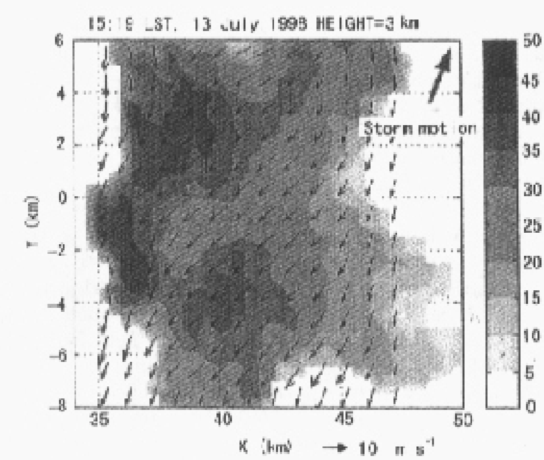

Fig. 2. Horizontal section of storm-relative wind and reflectivity fields at the 3 km level. This figure covers the area enclosed by the rectangle in Fig. 1.

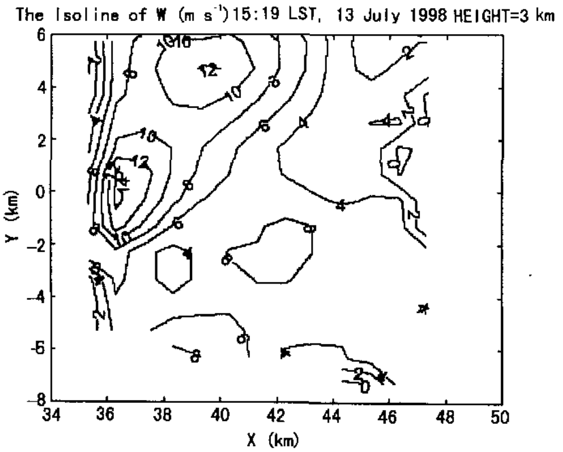

Fig. 3. The distribution of vertical speed w (m s^{-1}) at the 3 km level. Positive values stand for upward flow. This Figure covers the same area as Fig. 2.

2. Nonlinear approximation method

Let x be a vector in a finite dimensional space H. An approximation of x is usually defined by the action of a certain operator A_N on x such that $A_N x$ is close to x in some sense (for example, in the sense of a norm defined on H) and can be characterized by N parameters.

The approximation is said to be nonlinear if A_N is not a linear operator. In this paper, we are interested in the following nonlinear approximation technique.

Suppose that H is a Hilbert space and $\{e_k\}_k > 0$ is an orthonormal basis of H. We define for all $x \in H$ and $N > 0$,

$$A_N x = \sum_{k \in E_N} (x, e_k) e_k \,,$$

where $E_N = E_N(x)$ represents the set of indices corresponding to the N largest coordinates of x, i.e., Card $(E_N) = N$ and

$$k \in E_N, l \in E_N \Rightarrow |\langle x, e_k \rangle| < |\langle x, e_l \rangle|$$

The Reproducing Kernel Hilbert Spaces (RKHS) plays a central role in solving the function approximation problem. A RKHS is defined as a Hilbert space of functions defined over some domain $\Omega \subset R^d$ with the property that for each $x \in \Omega$, the evaluation functional F_x, defined as

$$F_x[f] = f(x), \forall f \in H$$

is a linear, bounded functional. It can be proved that we can associate to every RKHS, a positive definite function $K(x, y)$, which is called the reproducing kernel of H. This kernel of H has the following reproducing property

$$f(x) = \langle f(y), K(y, x) \rangle_H, \forall f \in H \,,$$

where $\langle ., . \rangle_H$ denotes the scalar product in H.

Consider a given observation set of N data points $\{x_k, y_k\}_{k=1}^N$ with input data $x_k \in R^n$ and output $y_k \in R$. The unknown function $f(x)$ is recovered or approximated from the given data. We assume that the function f underlying the data can be represented as

$$f(x) = \sum_{n=1}^{\infty} c_n \phi_n(x) + b \,,$$

where the linearly independent basis functions $\{\phi_n(x)\}_{n=1}^{\infty}$ are called features, and c_n and b are parameters to be estimated from the data. The problem of recovering the coefficients c_n and b from the data D is clearly ill-posed, since it has an infinite number of solutions. In order to make this problem well posed, regularization theory was proposed by Tikhonov and Arsenin (1977). Given a kernel K, the empirical risk minimization regularization theory framework suggests to minimize the following functional,

$$H[f] = \frac{1}{l} \sum_{i=1}^{l} \| y_i - f(x_i) \|_{L_2}^2 + \gamma \| f \|_K^2 \,,$$

where $\| \cdot \|_K$ is the norm in RKHS. Minimizing the first term is to guarantee a small actual risk with the error function $\frac{1}{l} \sum_{i=1}^{l} \| y_i - f(x_i) \|_{L_2}^2$, and the second smoothness, while γ controls the trade-off between these two terms.

3. Analyses for retrieving the wind field

We simply use the radial basis function (RBF) kernel,

$$K(x, x_i) = \exp(- \| x - x_i \|^2 / \delta) \,,$$

where δ is a given parameter. Let the kernel function K define the inner product in some implicit feature space with the associated transformation ϕ, which need not be computed explicitly. Hence,

$$K(x, y) = \phi(x) \cdot \phi(y)$$

We adopt a Cartesian reference frame $\{x, y, z\}$ where the radar is the origin (0, 0, 0) and z the vertical coordinate, and assume the vector representation of the motion of scatters $V = (u, v, w)$, which varies piecewise smoothly around its value (u_0, v_0, w_0) at a point (x_0, y_0, z_0). That is, the component of the wind vector will be expanded with respect to the basis function ϕ about the point (x_0, y_0, z_0),

$$u = \alpha^T \phi(x - x_0, y - y_0, z - z_0) \,, \qquad (1)$$

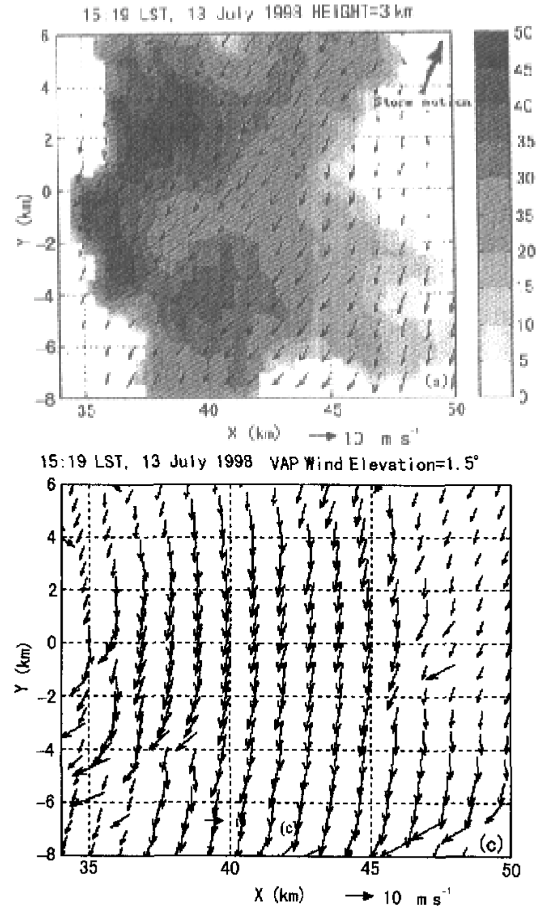

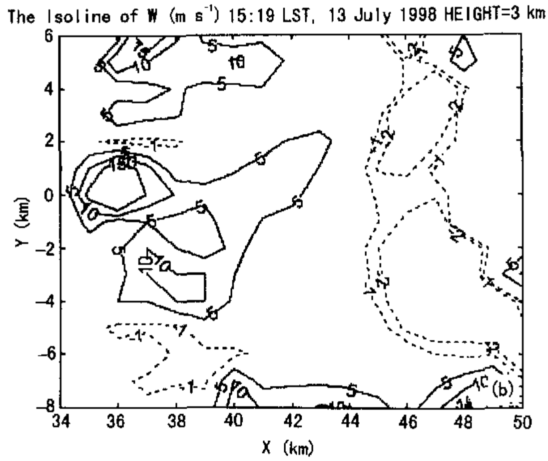

Fig. 4. (a) Horizontal section of storm-relative wind and reflectivity fields at the 3 km level by dual Doppler radar. (b) The distribution of vertical speed w (m s^{-1}) and reflectivity fields at the 3 km level. (c) Horizontal section of storm-relative wind by VAP method, elevation=1.5°. These figures cover the same area as Fig. 2..

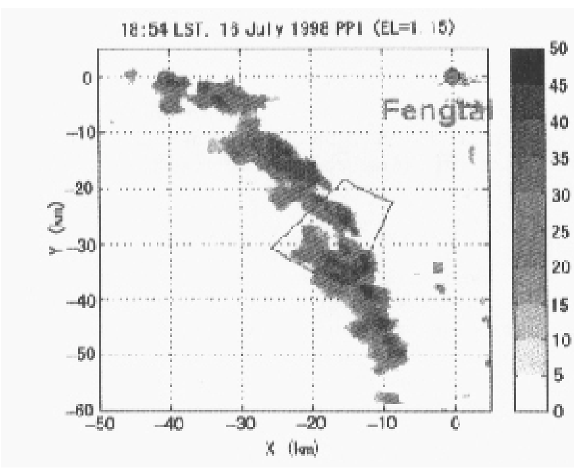

Fig. 5. The reflectivity (PPI, EL=1.15°) of the Fengtai radar at 1854 LST 16 July 1998.

where α is the corresponding coefficients vector and the same for v and w. Then the retrieved $\hat{V}_r$ can be obtained as following equation,

$$\hat{V}_r = -u\cos\theta\cos\phi - v\sin\theta\cos\phi - w\sin\phi\,, \qquad (2)$$

where θ and ϕ are the azimuth and elevation respectively. The radial velocity measured by the radar is V_r. Our purpose is to obtain a $\hat{V}_r$ such that

$$\| \hat{V}_r - V_r \| = \min\,. \qquad (3)$$

The problem of recovering the coefficients of Equation (1) from the radar radial measurement V_r is under-determined, so directly retrieving the wind field is impossible. However, with the piecewise smooth assumption of the wind field, it will be possible to retrieve the wind field. In fact, we can add the constraint as follows,

$$\| \alpha \| = \min\,. \qquad (4)$$

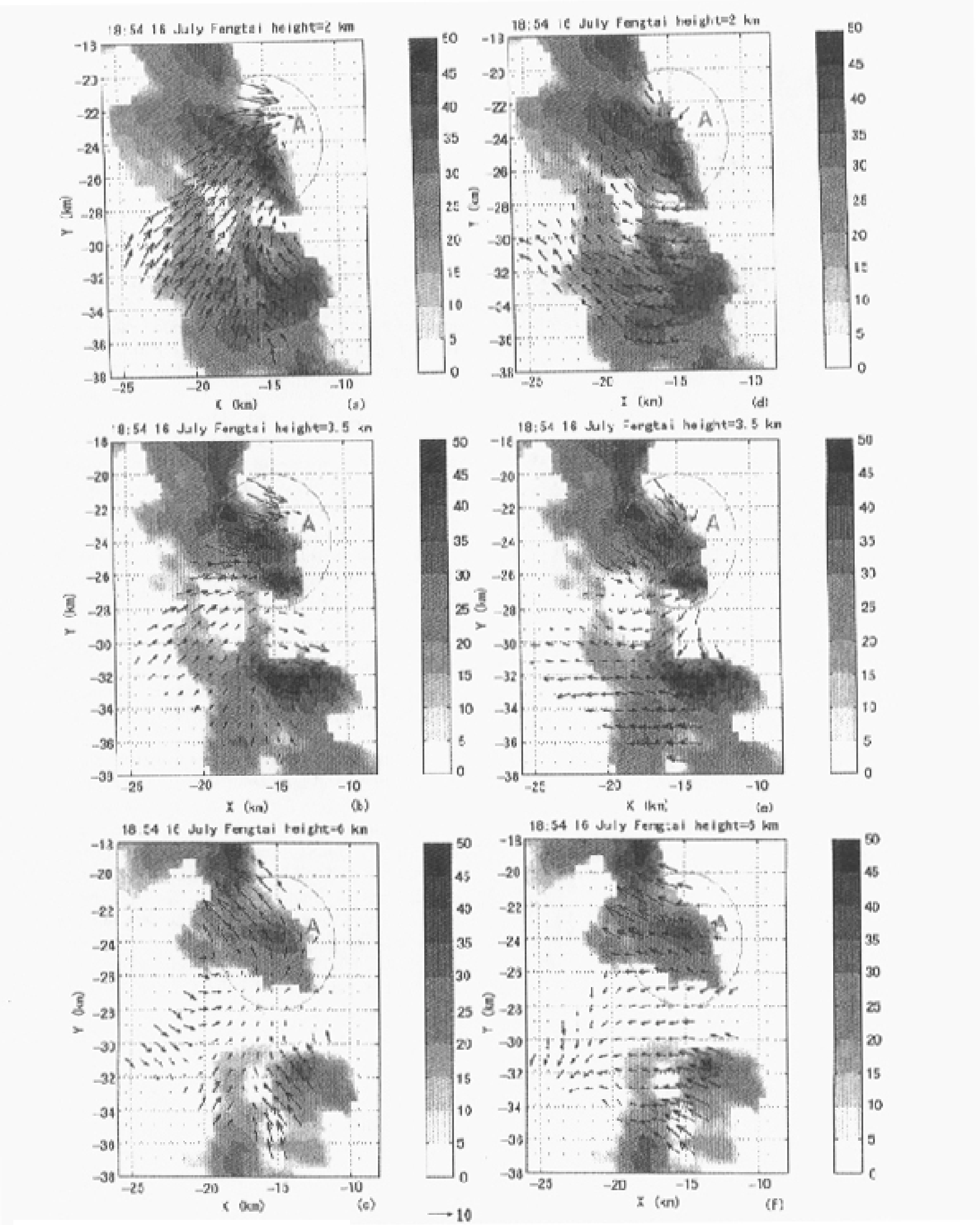

Fig. 6. (a)-(c) Horizontal section of wind and reflectivity at 2 km, 3.5 km, and 6 km height. (d)-(f) Horizontal section of storm-relative wind and reflectivity at 2 km, 3.5 km, and 6 km height.

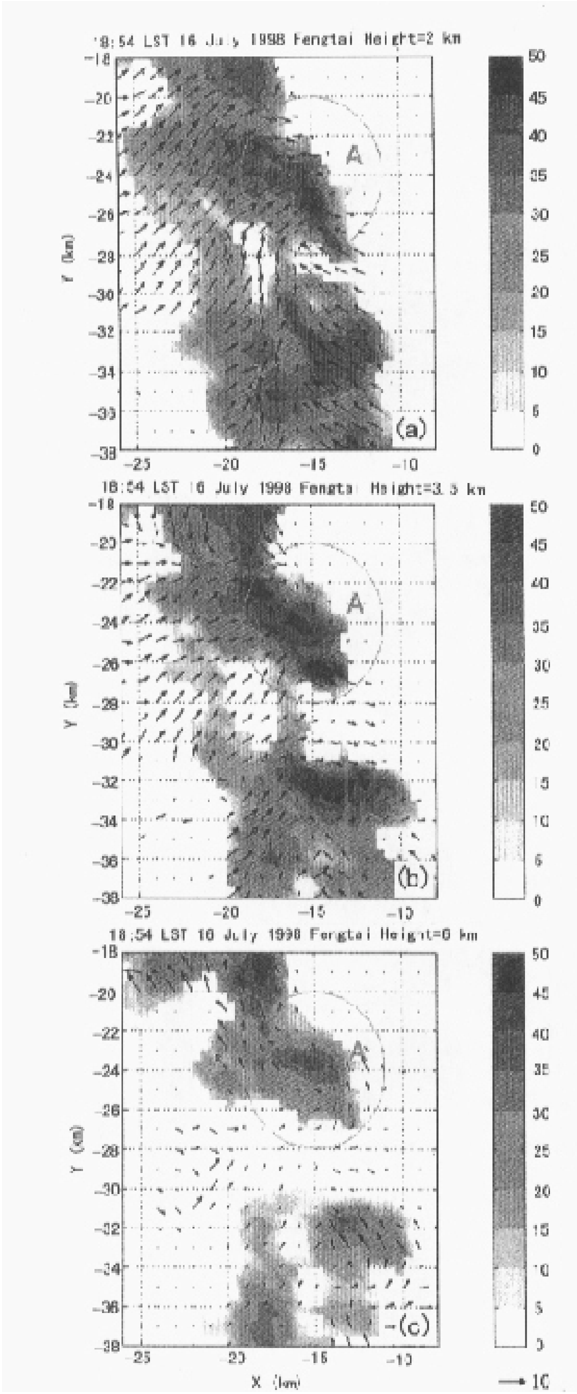

Fig. 7. Horizontal section of wind fields and reflectivity by dual Doppler radar at 2 km (a), 3.5 km (b), and 6 km (c) height.

4. Experiment

Now we use the method illustrated in sections 2 and 3 for two severe convective cases, and compare with the results previously obtained by dual or triple Doppler radar data.

4.1 *A deeply developed, long-lived cumulonimbus cloud*

The first retrieval experiment is made by Doppler radar data of Shouxian during 1517 LST 1523 LST on 13 July 1998. During this period, a deeply developed and long-lived cumulonimbus cloud was observed by triple Doppler radars, which were installed at Shouxian, Fengtai and Huainan in Anhui Province. Figure 1 shows the horizontal plane of the radar analysis for the cumulonimbus cloud. This convective radar-echo moved north-northeastward with a speed of 8 m s^{-1}. It was composed of several convective cells, among them the cell on the west side of the echo developed very deeply. Its echo-top height was maintained at higher than 14 km for about 1.5 h with a maximum height of 18.5 km. Meanwhile the intensive echo above 30 dBZ in the most developed cellular echo was found even above 15 km without change in the horizontal plane. In addition, this convective echo produced quite a large amount of precipitation. Takeda et al. (1999) and Shusse et al. (2000) revealed the three-dimensional kinetic structure of the cumulonimbus cloud by dual-Doppler radar analysis and retrieved the wind fields completely.

We use the NA method for retrieving the three-dimensional wind field from a single-Doppler radar observation. Figure 2 shows the horizontal section of storm-relative wind and reflectivity fields at 3 km of height at 1519 LST. The structure at this time is chosen as a typical one in the most intensive stage of this cumulonimbus cloud. From Fig. 2, we can see that the northeast wind prevails in the echo area and a convergence region exists along the west side of the intensive echo band, which implies an updraft area. Figure 3 shows the vertical speed w (m s^{-1}) at 3 km of height. The maximum speeds reach 14 m s^{-1} and 12 m s^{-1} respectively in Fig. 3 with Fig. 2, the most intensive echo region corresponds with the most intensive updraft region where the cumulonimbus cloud exists.

By comparing the results of the NA method (Figs. 2 and 3) with those of the dual-Doppler radar analysis in Fig. 4, it can be seen that the horizontal wind field retrieved by the NA method (Fig. 2) is very similar to the one by the dual-Doppler radar data (Fig. 4a). As for the vertical motion, the updraft flow regions (Fig. 3) agree well with the dual-Doppler analysis (Fig. 4b), while the downdraft flow regions in the eastern part of

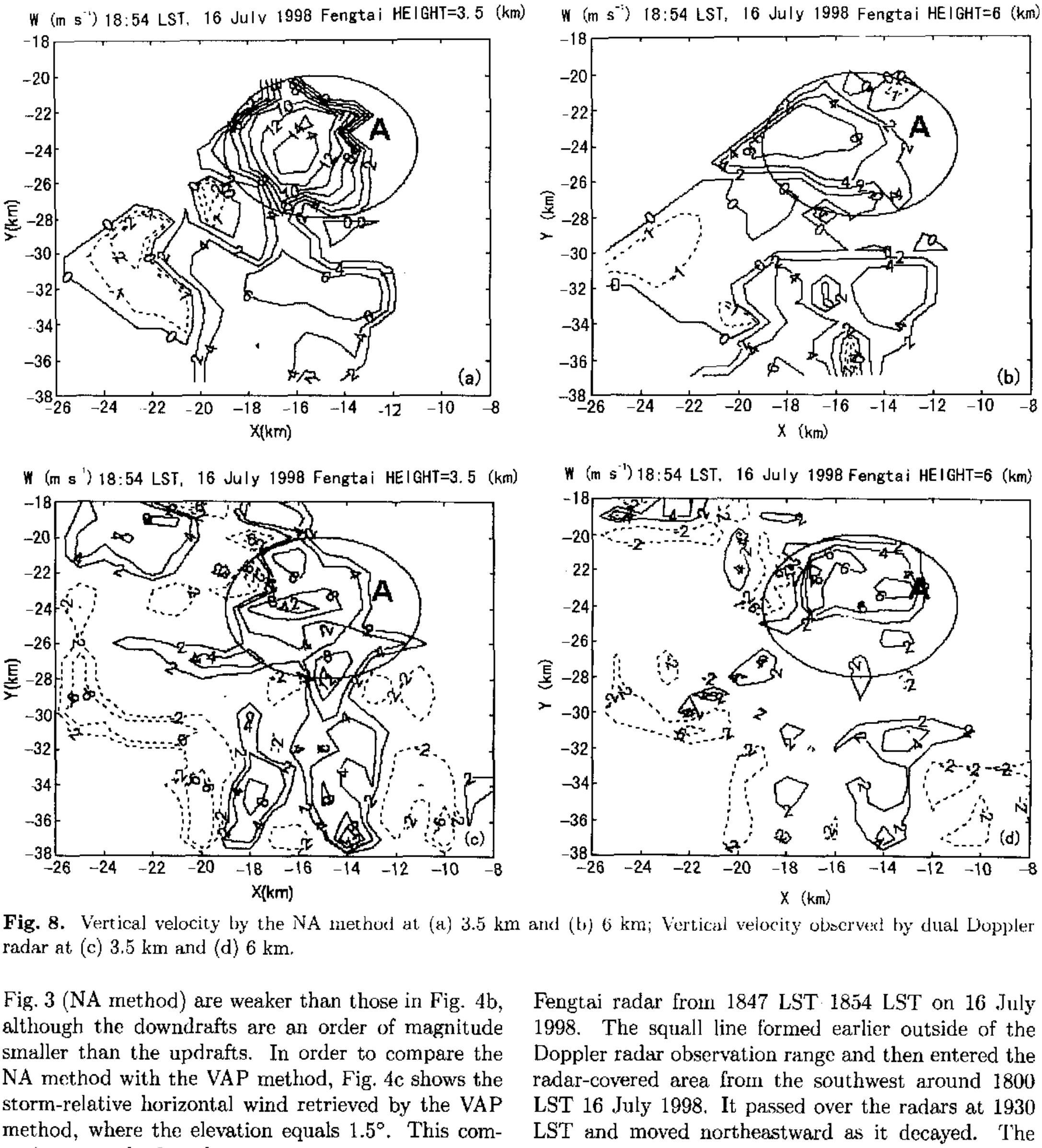

Fig. 8. Vertical velocity by the NA method at (a) 3.5 km and (b) 6 km; Vertical velocity observed by dual Doppler radar at (c) 3.5 km and (d) 6 km.

Fig. 3 (NA method) are weaker than those in Fig. 4b, although the downdrafts are an order of magnitude smaller than the updrafts. In order to compare the NA method with the VAP method, Fig. 4c shows the storm-relative horizontal wind retrieved by the VAP method, where the elevation equals 1.5°. This comparison reveals that the convergence region exists on the western edge of the echoes, but the convergence band from the northeast to the southwest is not as clear as those by the NA method or the and dual-Doppler analysis. This implies that the results from the NA method are to some degree better than those from the VAP method.

4.2 *A squall line*

The second case is a squall line observed by the Fengtai radar from 1847 LST–1854 LST on 16 July 1998. The squall line formed earlier outside of the Doppler radar observation range and then entered the radar-covered area from the southwest around 1800 LST 16 July 1998. It passed over the radars at 1930 LST and moved northeastward as it decayed. The squall line extended from the northwest to the southeast with a width of a few tens of kilometers. Figure 5 shows that the squall line consisted of intense convective cells and its leading edge was clear. Most of the convective cells were located along the leading edge with reflectivity above 40 dBZ, and some of the cells reached a height of 17 km. A box in the figure encloses the area for retrieval.

Figures 6a-c show the horizontal velocity at heights of 2 km, 3.5 km, and 6 km respectively, and Figs. 6d-f show the corresponding horizontal velocity relative to the squall line. It is clearly seen that the horizontal velocity at the height of 2 km prevails from the southwester and the convergence exists on the north side of the echoes indicated by the circle A. The southwesterly wind still prevails at 3.5 km, but at 6 km, the divergence is evident in the area A. By comparing the horizontal wind field from the NA method (Figs. 6a-c) with that from the dual-Doppler radar (Figs. 7a-c), it can be seen that the two are similar. Figures 8a-b show the vertical velocity at 3.5 km and 6 km from the NA method respectively. In the area A, where the echo is strong from 2 km up to 6 km, the air flow converges at lower levels and diverges at higher levels in the troposphere.

This means that upward motion evidently exists in this area, which can produce strong convective weather, and this structure is identical to the result analyzed by Ogura and Liou (1980). Figures 8c-d show the vertical velocity at 3.5 and 6 km respectively obtained from dual-Doppler radar data. By comparing Figs. 8a-b with Figs. 8c-d, it can be seen that the overall patterns are very similar to each other, especially for the strong upward motions in region A. But the downward motions located in the southwest of Figs. 8a-b are weaker than those in Figs. 8c-d, although the downdrafts are much smaller than the updrafts, as in the first case. Probably one of the reasons is that in the NA method, the continuity equation has not been included, yet in the constraints, it is possible to restrict the development of compensating downdrafts. This is a problem to be studied in the future.

5. Error analysis

In order to evaluate the NA method, we analyze the retrieved result based on the following statistics: the mean absolute percentage error of radial velocity (f_1), defined in Eq.(6); the mean radial velocity error (f_2), defined in Eq.(7). Variable σ_i is the absolute difference of radar observation radial velocity and retrieved radial velocity at point $i(x_0, y_0, z_0)$.

$$\sigma_i = | V_{r_i} - \hat{V}_{r_i} | \tag{5}$$

$$f_1 = \frac{1}{n} \sum_{i=1}^{n} | \frac{\sigma_i}{V_{r_i}} | \times 100\% \tag{6}$$

$$f_2 = \frac{1}{n} \sum_{i=1}^{n} \sigma_i \tag{7}$$

It is seen clearly in Fig. 9a that the mean absolute percentage error of radial velocity decreases with the increase of radial speed. When the radial speed is below 4 m s^{-1}, the error is above 30%; the maximum reaches 84%, which illustrates that the small radial speed has a higher error. From Fig. 9b, we can see that the mean radial velocity error is small (below 1.5 m s^{-1}) compared with the precision of the Doppler radar 1.0 m s^{-1}, which means the NA method is effective and the retrieved wind fields are close to the actual data. However, we find that both the mean absolute percentage error and mean radial velocity error fluctuate dramatically, which is probably due to the poor quality of some sampling points and the large sampling volume.

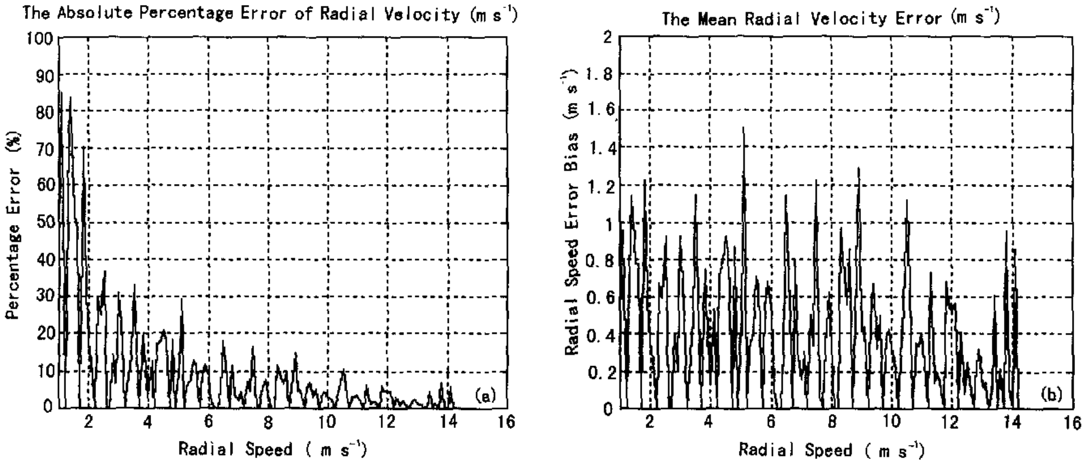

Fig. 9. (a) The mean absolute percentage error of radial velocity and (b) the mean radial velocity error as a function of radial speed. Positive value: upward motion; negative value: downward motion.

6. Conclusions

In this paper, the nonlinear approximation method is proposed and applied to retrieve the three-dimensional wind from single-Doppler radar observations. This method depends highly on the nonlinear (the small-scale irregularities) variation of the wind so that the retrieved wind structure can be revealed. Furthermore, the method can acquire a higher resolution (a high radar sampling resolution) wind field compared with previous methods such as the VVP method.

By comparing the retrieved results from the NA method with the observed wind field from dual-Doppler radar, one sees that the overall patterns are very similar between the two, especially for the areas of strong upward motion. But the magnitudes of the downward motions are weaker in the figures of the NA method than those of the dual-Doppler radar, although the downdrafts are obviously smaller than the updrafts in the dual-Doppler radar observations.

Since the nonlinear approximation method is newly introduced and newly applied to the retrieval of single-Doppler radar wind fields, thus, its advantages and deficiences need further investigation and improvement from this initial work.

Acknowledgments. The authors would like to express their thanks to the GAME/HUBEX Project Office for assistance.

REFERENCES

Bai J., Zhou X. B., Wang L. K., and Tao Z. Y., 2001: Error analysis of Doppler radar expanded VAD technique. *Acta Scientiarum Naturalium Universitatis Pekinensis*, **37**(1), 48–54.

Bai J., and Tao Z. Y., 2000: The pre-processing of Doppler radar wind retrieval VAP technique. *Quarterly Journal of Applied Meteorology*, **11**(1), 21–26. (in Chinese)

Bluestin, H., and D. Hazen, 1989: Doppler radar analysis of a tropical cyclone over land: Hurricane Alicia (1983) in Oklahoma. *Mon. Wea. Rev.*, **117**, 2594–2611.

Boccippio, D. J. 1995: A diagnostic analysis of the VVP single-Doppler retrieval technique. *Journal of Atmospheric and Oceanic Technology*, **12**, 230–248.

Browning, K. A., and R. Welxler, 1968: The determination of kinematic properties of a wind field using Doppler radar. *J. Appl. Meteor.*, **7**, 105–113.

Chapelle, O., P. Haffner, and V. N. Vapnik, 1999: Support vector machines for histogram-based image classification. *IEEE Trans. Neural Networks*, **10**, 1055–1064.

Cohen, A., and J. d'Ales, 1997: Nonlinear approximation of random functions. *SIAM J. Appl. Math*, **57**, 518–540.

Coifman, R. B., Y. Meyer, and V. M. Wickerhauser, 1992: Entropy-based algorithms for best basis selection. *IEEE Transactions on Information Theory*, **38**(2), 713–718.

Evgeniou T., 2000: Statistical learning theory: A primer. *International Journal of Computer Vision*, **38**(1), 9–13.

Girosi, F., 1998: An equivalence between sparse approximation and support vector machines, 1998: *Neural Computation*, **10**(6): 1455–1480.

Gorodnitsky, I. F., and B. D. Rao, 1997: Sparse signal reconstruction from limited data using FOCUSS: A re-weighted minimum norm algorithm. *IEEE Trans. Signal Processing*, **45**, 600–616.

Johnston, B. W., J. D. Marwitz, and R. Carbone, 1990: Single Doppler radar analysis of banded precipitation structures. *J. Atmos. Oceanic Technol.* **7**(6), 866–875.

Tsuboki, K., B. Geng, and T. Takeda, 2000: Dual Doppler radar analysis of a squall line observed over the China continent during the HUBEX intensive field observation, International GAME/HUBEX Workshop, 12–14 September, Sapporo JAPAN, 69–75.

Klimowski, B. A., and J. D. Marwitz, 1990: Single Doppler analysis of a severe squall line. Preprints, 16th Conf. on Severe Local Storms, Kananaskis, Alberta. *Amer. Meteor. Soc.*, 252–255.

Lhermitte, R. M., and D. Atlas, 1961: Precipitation motion by pulse Doppler. Proc., Ninth Weather Radar Conf., Boston. *Amer. Meteor. Soc.*, 218–223.

Liou, Y. C., Gal-Chen, and D. K. Lilly, 1991: Retrieval of wind temperature and pressure from single-Doppler radar and a numerical model, 25th International Conf. on Radar Meteorology, Paris. *Amer. Meteor. Soc.*, 151–154.

Liu S. Y., and Z. Y. Tao, 1999: The Retrieval of the horizontal divergence field from a single-Doppler radar velocity field. *Quarterly Journal of Applied Meteorology*, **10**(1), 41–48. (in Chinese)

Marwitz, J. D., and R. Carbone, 1990: Single Doppler analysis of banded precipitation structures. *J. Atoms. Oceanic Technol.*, **7**, 866–875.

Marwitz, J. D., 1990: A case study of heavy snowfall in Oklahoma. Preprints, Fourth Conf. on Mesoscale Processes, Boulder. *Amer. Meteor. Soc.*, 61–62.

Matejka, T., and R. C. Srivastava, 1991: An improved version of the extended velocity-azimuth display technique for analyzing single-Doppler radar data. *J. Atmos. Oceanic. Technol.*, **8**, 453–466.

Ogura, Y., and M. T. Liou, 1980: The structure of a mid-latitude squall line: A case study. *J. Atmos. Sci.*, **37**, 553–567.

Peace, R. L., R. A. Brown, and H. G. Camnitz, 1969: Horizontal motion field observations with a single pulse Doppler radar. *J. Atmos. Sci.*, **26**, 1096–1103.

Qiu, C. J., and Q. Xu, 1992: A simple adjoint method of wind analysis for single-Doppler data. *J. Atmos. Oceanic Technol.*, **9**, 588–598.

Scialom, G., and J. Testud, 1986: Retrieval of horizontal wind field and mesoscale vertical vorticity in stratiform precipitation by conical scanning with Doppler radars. *J. Atmos. Oceanic Technol.*, **3**, 696–703.

Shusse, Y., H. Minda, B. Geng, K. Tsuboki, and T. Takeda, 2000: Three-dimensional airflow structure of deeply developed long-lived cumulonimbus cloud in the atmospheric situation of weak vertical wind shear, International GAME/HUBEX Workshop, 12–14 September, Sapporo JAPAN, 76–77.

Smythe, G. R., and D. S. Zrnic, 1983: Correlation analysis of Doppler radar data and retrieval of the horizontal wind. *J. Climate Appl. Meteor.*, **22**, 297–311.

Srivastava, R. C., T. J. Matejka, and T. J. Lorello, 1986: Doppler radar study of the trailing anvil region associated with a squall line. *J. Atmos. Sci.*, **43**, 356–377.

Sun, J., D. W. Flicker, and D. K. Lilly, 1991: Recovery of three-dimensional wind and temperature fields from single-Doppler radar data. *J. Atmos. Sci.*, **48**, 876–890.

Suykens, J. A. K., L. Lukas, and J. Vandewalle, 1999: Sparse approximation using least squares Support vector machine. Internal Report 99-84, ESAT SISTA, K. U. Leuven (Leuven, Belgium) Accepted for publication in *Proc. of the IEEE International Symposium on Circuits and Systems* (*ISCAS 2000*), Geneva, Switzerland, May 2000, 757–760.

Takeda, T., Y. Shusse, H. Minda, Y. Wakatsuki, B. Geng, and K. Tsuboki, 1999: Three-dimensional structure of deeply developed long-lived cumulonimbus cloud in the HUBEX IFO, Workshop on Meso-scale Systems in Meiyu/Baiu Front and Hydrological Cycle, 3–9 November, Xi'an, China, 79–80.

Tao Z. T., 1992: The VAP method to retrieve the wind vectors field based on single-Doppler velocity field. *Acta Meteor. Sinica*, **50**, 81–90. (in Chinese)

Tikhonov, A. N., and V. Y. Arsenin, 1977: *Solutions of Ill-posed Problems*. W. H. Winston. Washington, D. C.: 224pp.

Tuttle, J. D., and G. B. Foote, 1990: Determination of the boundary layer airflow from a single-Doppler radar. *J. Atmos. Oceanic Technol.*, **7**, 218–232.

Vapnik, V. N., 1995: *The Nature of Statistical Learning Theory*. Springer-Verlag, New York., 188pp.

Vapnik, V. N., 1998a: *Statistical Learning Theory*. Wiley, New York, 732pp.

Vapnik, V. N., 1998b: The support vector method of function estimation. *Nonlinear Modeling: Advanced Blackbox Techniques*, J. A. K. Suykens, and J. Vandewalle, Eds., Kluwer Academic Publishers, Boston, 55–85.

Vapnik, V. N., and A.Y. Chervonenkis, 1971: On the uniform convergence of relative frequencies of events to their probabilities. *Theory of Probability and Its Applications*, **17**(2), 264–280.

Vapnik, V. N., and S. Mukherjee, 2000: Support vector method for multivariate density estimation. *Advances in Neural Information Processing Systems 12*, S. A. Solla, T. K. Leen, and K. -R. Muller, Eds., MIT Press Cambridge, Massachusetts, 659–665.

Waldteufel, P., and H. Corbin, 1979: On the analysis of single-Doppler radar data. *J. Appl. Meteor.*, **18**, 532–542.

Wei M., Dang R. Q., Ge W. Z., and T. Takeda, 1998: Retrieval of single-Doppler radar wind with variational assimilation method, Part I: Objective selection of functional weightings factors. *Advances in Atmospheric Sciences*, **15**, 533–568.

Xin, L., and G. W. Reuter, 1998: VVP technique applied to an Alberta storm. *J. Atmos. Oceanic Technol.*, **15**, 587–592.

Xu Q., and C. J. Qiu, 1994: Simple adjoint methods for single-Doppler wind analysis with strong constraint of mass conservation. *J. Atmos. Oceanic Technol.*, **11**, 289–298.

Xu, Q., C. J. Qiu, H. D. Gu, and J. X. Yu, 1995: Simple adjoint retrieval of microburst winds from single-Doppler radar data. *Mon. Wea. Rev.*, **123**, 1822 1833.

用非线性近似方法反演单多普勒雷达风场

赵 坤 刘国庆 葛文忠 党人庆 Takao TAKEDA

摘 要

回顾了近年来由单多普勒雷达观测反演风场的各种方法。这些方法大部分基于线性假设，因此风场的非线性变化经常影响反演结果，使得反演的风场误差增大。我们提出一种以非线性近似理论为基础的反演方法，该方法主要考虑了风场分片光滑的特点并充分利用了雷达的径向风场数据。我们把该方法应用到1998年淮河能量与水循环实验的两个个例中。通过同双多普勒雷达观测的结果比较，发现该方法能反演较高分辨率和准确性的水平风场，反演的垂直风场也比较合理。

关键词：非线性近似，分片光滑，基函数